Available online at www.sciencedirect.com
SCIENCE DIRECT®
ELSEVIER
Nuclear Instruments and Methods in Physics Research A 521 (2004) 454–467
NUCLEAR INSTRUMENTS & METHODS IN PHYSICS RESEARCH Section A
www.elsevier.com/locate/nima

New experimental validation of the pulse height weighting technique for capture cross-section measurements

U. Abbondanno[a], G. Aerts[b], H. Alvarez[c], S. Andriamonje[b], A. Angelopoulos[d], P. Assimakopoulos[e], C.O. Bacri[f], G. Badurek[g], P. Baumann[h], F. Bečvář[i], H. Beer[j], J. Benlliure[c], B. Berthier[f], E. Berthomieux[b], S. Boffi[k], C. Borcea[l], E. Boscolo-Marchi[m], N. Bustreo[m], P. Calviño[n], D. Cano-Ott[o], R. Capote[p], P. Carlson[q], P. Cennini[l], V. Chepel[r], E. Chiaveri[l], C. Coceva[s], N. Colonna[t], G. Cortes[n], D. Cortina[c], A. Couture[u], J. Cox[u], S. Dababneh[j], M. Dahlfors[l], S. David[f], R. Dolfini[k], C. Domingo-Pardo[v], I. Duran[c], C. Eleftheriadis[w], M. Embid-Segura[o], L. Ferrant[f], A. Ferrari[l], L. Ferreira-Lourenco[x], R. Ferreira-Marques[r], H. Frais-Koelbl[y], W.I. Furman[z], Y. Giomataris[b], I.F. Goncalves[x], E. Gonzalez-Romero[o], A. Goverdovski[aa], F. Gramegna[m], E. Griesmayer[y], F. Gunsing[b], R. Haight[ab], M. Heil[j], A. Herrera-Martinez[l], K.G. Ioannides[e], N. Janeva[ac], E. Jericha[g], F. Käppeler[j], Y. Kadi[l], D. Karamanis[e], A. Kelic[h], V. Ketlerov[aa], G. Kitis[w], P.E. Koehler[ad], V. Konovalov[z], E. Kossionides[ae], V. Lacoste[l], H. Leeb[g], A. Lindote[r], M.I. Lopes[r], M. Lozano[p], S. Lukic[h], S. Markov[ac], S. Marrone[t], J. Martinez-Val[af], P. Mastinu[m], A. Mengoni[l], P.M. Milazzo[a], E. Minguez[af], A. Molina-Coballes[p], C. Moreau[f,a], F. Neves[r], H. Oberhummer[g], S. O'Brien[u], J. Pancin[b], T. Papaevangelou[w], C. Paradela[c], A. Pavlik[ag], P. Pavlopoulos[ah], A. Perez-Parra[o], J.M. Perlado[af], L. Perrot[b], V. Peskov[q], R. Plag[j], A. Plompen[ai], A. Plukis[b], A. Poch[n], A. Policarpo[r], C. Pretel[n], J.M. Quesada[p], M. Radici[k], S. Raman[ad], W. Rapp[j], T. Rauscher[ah], R. Reifarth[ab], F. Rejmund[f], M. Rosetti[s], C. Rubbia[k], G. Rudolf[h], P. Rullhusen[ai], J. Salgado[x], E. Savvidis[w], J.C. Soares[x], C. Stephan[f], G. Tagliente[t], J.L. Tain[v,*], C. Tapia[n], L. Tassan-Got[f], L.M.N. Tavora[x], R. Terlizzi[t], M. Terrani[k], N. Tsangas[aj], G. Vannini[ak], P. Vaz[x], A. Ventura[s], D. Villamarin-Fernandez[o], M. Vincente-Vincente[o], V. Vlachoudis[l], R. Vlastou[k], F. Voss[j], H. Wendler[l], M. Wiescher[u], K. Wisshak[j], L. Zanini[l]

*Corresponding author. Instituto de Física Corpuscular, CSIC-Univ. Valencia, Valencia, Spain. Tel.: +34-963864581; fax: +34-963864583.

E-mail address: jose.luis.tain@ific.uv.es (J.L. Tain).

0168-9002/$ - see front matter
doi:10.1016/j.nima.2003.09.066

[a] Instituto Nazionale di Fisica Nuclear-Sezione di Trieste, Italy
[b] CEA/Saclay - DSM/DAPNIA/SPhN, Gif-sur-Yvette, France
[c] Universidade de Santiago de Compostela, Spain
[d] Astro-Particle Consortium, University of Athens, Greece
[e] Astro-Particle Consortium, University of Ioannina, Greece
[f] Centre National de la Recherche Scientifique/IN2P3 - IPN, Orsay, France
[g] Atominstitut der Österreichischen Universitäten, Technische Universität Wien, Austria
[h] Centre National de la Recherche Scientifique/IN2P3 - IreS, Strasbourg, France
[i] Charles University, Prague, Czech Republic
[j] Forschungszentrum Karlsruhe GmbH, Institut für Kernphysik, Germany
[k] Università degli Studi Pavia, Italy
[l] CERN, Geneva, Switzerland
[m] Instituto Nazionale di Fisica Nucleare, Laboratori Nazionali di Legnaro, Italy
[n] Universitat Politècnica de Catalunya, Barcelona, Spain
[o] Centro de Investigaciones Energéticas Medioambientales y Tecnológicas, Madrid, Spain
[p] Universidad de Sevilla, Spain
[q] Kungliga Tekniska Hogskolan, Physics Department, Stockholm, Sweden
[r] Laboratorio de Instrumentacao e Phisica Experimental de Particulas, Coimbra, Portugal
[s] ENEA, Bologna, Italy
[t] Instituto Nazionale di Fisica Nuclear-Sezione di Bari, Italy
[u] University of Notre Dame, USA
[v] Instituto de Física Corpuscular, CSIC-Univ. Avda. Dr. Moliner 50, Bujassot, Valencia 46100, Spain
[w] Astro-Particle Consortium, University of Thessaloniki, Greece
[x] Instituto Tecnológico e Nuclear, Lisboa, Portugal
[y] Fachhochschule Wiener Neustadt, Wien, Austria
[z] Frank Laboratory of Neutron Physics, Joint Institute for Nuclear Research, Dubna, Russia
[aa] Institute of Physics and Power Engineering, Obninsk, Russia
[ab] Los Alamos National Laboratory, New Mexico, USA
[ac] Institute for Nuclear Research and Nuclear Energy, Sofia, Bulgaria
[ad] Oak Ridge National Laboratory, Physics Division, Oak Ridge, USA
[ae] Astro-Particle Consortium, NCSR "Demokritos", Athens, Greece
[af] Universidad Politécnica de Madrid, Spain
[ag] Institut für Isotopenforschung und Kernphysik, Universität Wien, Austria
[ah] University of Basel, Switzerland
[ai] CEC-JRC-IRMM, Geel, Belgium
[aj] Astro-Particle Consortium, University of Thrace, Greece
[ak] Dipartamento di Fisica and INFN, Bologna, Italy

The n_TOF Collaboration

Received 24 June 2003; accepted 30 September 2003

Abstract

The accuracy of the pulse height weighting technique for the determination of neutron capture cross-sections is investigated. The technique is applied to measurements performed with C_6D_6 liquid scintillation detectors of two different types using capture samples of various dimensions. The data for well-known (n, γ) resonances are analyzed using weighting functions obtained from Monte Carlo simulations of the experimental set-up. Several causes of systematic deviation are identified and their effect is quantified. In all the cases measured the reaction yield agrees with the standard value within 2%.

PACS: 25.40.Lw; 25.40.Ny; 29.40.Mc; 07.05.Tp

Keywords: Pulse height weighting technique; C_6D_6 scintillation detectors; Monte Carlo simulations; Neutron capture cross-sections

1. Introduction

There has been in recent times a renewed interest in high accuracy neutron cross-section data. The sources of this interest are to be found in the field of nuclear technology, in particular in relation to the concept of Accelerator Driven Systems (ADS) and the transmutation of nuclear waste, and in the field of Nuclear Astrophysics. In those disciplines the need has arisen to explore new regions of the nuclear chart and/or new energy regimes where scarce or discrepant data exists, or simply it was found that the precision of existing data does not suffice. The n_TOF experiment at CERN [1], has the aim of obtaining high-quality data relevant to both fields of research as well as to basic nuclear physics. Radiative capture measurements on a series of key isotopes with improved accuracy down to 2–3% are an important part of the planned experimental programme. These measurements will be performed by the method of counting the number of capture γ-ray cascades as a function of the neutron time of flight, allowing energy differential cross-section determinations in the neutron energy range from about 1 eV to 1 MeV. In the first phase such experiments are carried out using a set of a few C_6D_6 liquid scintillation detectors. In the second phase a 40 BaF_2-crystal Total Absorption Calorimeter (TAC), presently under construction, will be employed. The more complex and costly TAC will allow the measurement of some essential radioactive and rare material samples. On the other hand the lower neutron sensitivity of the C_6D_6 detectors is of advantage for the measurement of samples with a high neutron scattering to capture ratio. However, in this case the simplicity of the experimental set-up is counterbalanced by the more involved analysis procedure, the so-called Pulse Height Weighting Technique (PHWT), which requires the "a posteriori" manipulation of the previously determined detector response function.

The goal of a few percent accuracy on the (n,γ) cross-sections can only be achieved when all the sources of systematic uncertainties are well under control. This triggered a detailed investigation of the sources of error associated with the principles of the PHWT itself, in particular of the use of Monte Carlo (MC) simulations to model the detector response. In Section 2, we present in abbreviated form the results of our previous studies [2], supporting the conclusion that indeed the necessary degree of accuracy could be attained. Therefore it was decided to dedicate a part of the available beam time, after the commissioning of the installation, to its experimental verification. For this purpose a selected set of test measurements was performed using the experimental apparatus available at n_TOF. The relevant details of those measurements are described in Section 3. The data analysis procedure and the results obtained are presented in Section 4. Section 5 summarizes the conclusions.

2. Pulse height weighting technique issues

The PHWT is based on an original idea from Maier-Leibnitz [3] and requires the use of a low-efficiency γ-ray detector, such that one and only one γ-ray out of the capture cascade is registered at a time (condition I), but with detection efficiency ε_γ proportional to the photon energy E_γ (condition II):

$$\varepsilon_\gamma = \alpha E_\gamma. \tag{1}$$

Under these conditions the efficiency for detecting a cascade ε_c will be proportional to the known cascade energy and independent of the actual cascade path

$$\varepsilon_c = \sum_j \varepsilon_{\gamma_j} = \alpha E_c. \tag{2}$$

Apart from the detection of background counts (i.e. counts not related to sample capture γ-rays), condition I is affected by several sources of error: (a) the detection of more than one γ-ray per cascade, (b) the loss of cascade γ-rays due to the electron conversion process, and (c) the loss of cascade γ-rays due to noise rejecting thresholds. All three types of systematic error are best considered together, and can be estimated by the MC method as will be explained later.

Condition II, i.e. the proportionality of the efficiency with the γ-ray energy is achieved through the manipulation of the detector energy

response distribution $R(E)$ (or its energy binned equivalent R_i) by the introduction of a "pulse height" (i.e. deposited energy) dependent weighting factor $W(E)$, which is to be applied to each registered count. The smooth (in practice polynomial) dependence of the weighting factor on the energy is determined by a least-squares fit to a number of γ-ray responses in the energy range of interest (up to about 10 MeV)

$$\min \sum_j \left(\sum_i W_i R_i^j - \alpha E_{\gamma_j} \right)^2 . \quad (3)$$

Obviously, the adequacy of the Weighting Function (WF) employed, is the most conspicuous source of systematic error of the PHWT.

Historically, the detector response distributions needed to calculate the weighting factors were initially obtained from MC simulations, due to the difficulty of obtaining mono-energetic γ-ray sources in the energy range of interest. In the early 80s a serious discrepancy was found between the neutron width Γ_n obtained by capture measurements using the PHWT and the one obtained from transmission measurements for the well-known 1.15 keV resonance in ^{56}Fe. After thorough investigations it became clear that the problem had its origin in the MC-simulated response distributions.

This conclusion was mainly supported by careful measurements at Geel [4] of mono-energetic γ-ray responses up to 8.4 MeV. The method employed was the coincidence technique for two-gamma cascades populated in (p,γ) resonance reactions in light nuclei. The measurements were performed with a detector arrangement employed in the (n,γ) measurements plus a high-resolution Ge detector for tagging one of the two γ-rays. The reaction target consisted of a thin material deposit on a 0.3 mm Ta backing. The extracted experimental WF when applied to the capture data on thin samples (0.5 mm) gave a cross-section in agreement with the standard transmission value for the 1.15 keV resonance in ^{56}Fe. Therefore, it was proposed to use the (p,γ) WF for the (n,γ) measurements. However it was also recognized that the cause of the discrepancy between the MC-simulated response and the measurement was due to the large influence of the materials surrounding the source which produce secondary radiation. This includes the sample under study itself, casting doubts on the universality of the WF so determined. In fact the MC method seems the only practical method to take into account the systematic differences of the various sample/detector arrangements. At Oak Ridge [5] the MC method was further investigated and it was found that the EGS4 code [6] gave a satisfactory Γ_n value for the 1.15 keV resonance in ^{56}Fe measured with their experimental capture set-up using samples of 0.5 mm and 1.2 mm thickness. However [4], they were not able to produce the same result for the data measured with the Geel set-up.

In view of this unclear situation we have re-investigated the issue of the accuracy of the MC simulations, in particular whether the differences between simulation and measurement could be due to insufficient detail in the description of the measuring set-up or rather due to a poor implementation in the MC code of the relevant physical processes in the generation and interaction of the secondary radiation. The simulation package GEANT3 [7] was chosen based on our previous successful experience with it and its capability of defining complex geometries. The code was used to extensively investigate the response of the (p,γ) experimental set-up described in Ref. [4] in the photon energy range 1.2–8.4 MeV. The detailed geometric description of the beam line, target and detectors was reproduced in the simulation. The main results of this study can be summarized as follows [2]:

(1) The shape of the measured response distribution is well reproduced by the simulation throughout the whole γ-ray energy range. The absolute value of the efficiency is well reproduced at the higher energies but there is a tendency to overestimate it at low energies, by up to 18% at 1.2 MeV. The same behaviour was obtained when the MCNP [8] simulation code was employed. The reason for this discrepancy is not clear.
(2) At high γ-ray energies the contribution to the detection efficiency of the secondary radiation produced in the dead materials is very large: close to 40% around 8 MeV. The contribution

of the detector dead material itself is negligible compared with the contribution of the (p,γ) target backing (0.3 mm thick Ta plate) in this set-up. Therefore, the experimentally determined weighting function could produce erroneous results depending on the sample.

The latter point was verified experimentally by Fioni et al. [9] by comparing the PHWT result for the 1.15 keV resonance in ^{56}Fe using the experimental WF of Ref. [4] for samples of different thicknesses and compositions: 0.5, 1.0, and 1.5 mm Fe samples, a 4.1 mm Fe_2O_3 sample, and a sandwich of five Fe samples with four Au samples totalling a thickness of 2.2 and 0.6 mm respectively. All samples were 8 cm in diameter. The measurements for the single metallic and oxide samples were normalized to the measurement of the 4.9 eV resonance in ^{197}Au performed with a 0.1 mm thick Au sample, while the sandwich sample provides self-calibration. The neutron width Γ_n extracted in Ref. [9] from the capture measurement, normalized to the standard transmission value, is shown in Fig. 1 (triangles). This figure clearly illustrates the complex dependency of the extracted result on sample thickness and composition: the thick sandwich sample (2.2 mm Fe) gives a result in agreement with the transmission value as well as the thinner metallic samples (0.5 and 1.0 mm), while the 1.5 mm metallic sample and the Fe_2O_3 sample clearly deviate. This lead the authors to recommend the use of the experimental WF only for thin samples. However we should point out that some of the planned measurements at n_TOF would require the use of rather thick samples in order to keep the amount of beam time within reasonable limits.

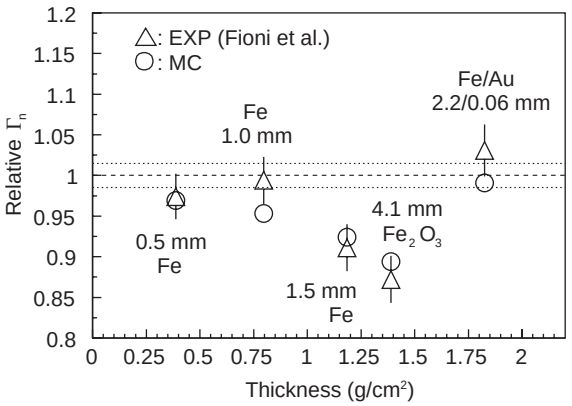

Fig. 1. Comparison of the neutron widths for the 1.15 keV resonance in ^{56}Fe obtained with the PHWT using several samples. Values are normalized to the reference transmission value $\Gamma_n = 61.7(9)$ meV. Triangles: experimental values from Ref. [9], circles: MC simulation.

In addition to showing the limitations of the WF from Ref. [4], the detailed experimental information of Ref. [9] gave us the possibility of performing an indirect check of the accuracy of our MC simulation. This was achieved by performing a simulation of the measurement itself and applying to the simulated deposited energy spectra the experimental WF of Ref. [4]. In order to have a realistic simulation of the measurement, capture cascades of appropriate energy and multiplicity distribution have to be generated for the ^{197}Au and ^{56}Fe resonances. The statistical model of the nucleus provides such a possibility through the application of the MC method as is detailed in Ref. [2]. The result of the simulated experiment (circles) is compared to the measurement in Fig. 1. As can be observed the simulation reproduces closely the staggering of the experimental points. That is to say, the simulation reproduces the differences in the response functions for the different set-ups, while the experimental WF cannot. Obviously if the simulated measurements were analyzed with the simulated WF in each case all the values would be consistent with the transmission value, giving a strong indication that indeed a few percent accuracy could be achieved with the PHWT.

Following these considerations it was found pertinent to perform a direct verification of the degree of accuracy which can be achieved with the PHWT using MC-based WF, carrying out several measurements of the particularly sensitive 1.15 keV resonance in ^{56}Fe using different sample sizes and experimental set-ups, which were anticipated will be used at the n_TOF installation, as is described in the following sections.

3. Experiment

At n_TOF much attention has been paid to the minimization of the intrinsic neutron background

of the installation through a careful shielding design. Despite these efforts the neutron sensitivity of the detectors is of concern since the measured sample itself becomes a source of background neutrons through scattering. Two different sets of C_6D_6 detectors with different neutron sensitivities have been developed at n_TOF for capture experiments [10]:

(a) a set of four commercial BICRON detectors modified for low neutron sensitivity, with thinned Al capsule walls (front wall 1.0 mm, side wall 0.4 mm), removable TEFLON expansion tubing and a Photonis XP1208 boron-free glass window photomultiplier tube (PMT). The 0.6l liquid scintillator cell (76.2 mm × 101.6 mm ∅) is enclosed by a 9.5 mm thick quartz window.

(b) a set of two carbon fibre cell detectors (wall thickness: 0.4 mm) with no quartz window for ultra low neutron sensitivity with a volume of 1.0l (78 mm × 127.3 mm ∅) assembled at Forschungszentrum Karlsruhe (FZK). The PMT used was the model 9823 from EMI with a quartz window.

Since both types of detector are envisaged for use in capture measurements they were both employed in the test measurements.

The standard capture experimental set-up includes a carbon fibre sample changer [11] which allows the placement under vacuum of up to 10 different samples in the neutron beam through remote control. Carbon fibre was preferred to aluminium (a) because the latter has a resonance-dominated capture cross-section for background neutrons and (b) to minimize the influence of dead material close to the sample on the detector photon response according to the findings of the MC study reported in Section 2. A horizontal beam tube of 1 m length and 50 mm inner diameter is crossed vertically by a 1 m long and 80 mm inner diameter tube containing the movable sample holder. Both tubes have a thickness of 2 mm. The sample holder is 1 m long, 7 cm wide and 0.4 mm thick, with ten 5 cm diameter holes made every 10 cm for the samples. The samples themselves are placed in the centre of a 7 cm × 7 cm × 0.6 mm frame with a 5 cm diameter hole using a thin Kapton foil.

The neutron beam profile [12] at the sample position (at $L = 185.05$ m from the proton spallation target) is limited to a diameter of 4 cm by the collimators in use and has an approximate Gaussian shape with $\sigma = 7$ mm, slightly off centred ($\Delta_x = 1.5$ mm) in the horizontal direction. Therefore the standard sample diameter is chosen as 4.5 cm, but for low mass samples, smaller diameters of about 2 cm are chosen in order to optimize the reaction yield.

Two different sets of measurements, separated in time, were carried out, each using one of the above-mentioned detector types (BICRON and FZK in short). In each case, two detectors were placed in horizontal position at $\theta = 90^\circ$ on each side of the neutron beam and close to the sample changer vertical tube, in such a way that the distance to the centre of the sample was $d \simeq 4.2$ cm. The detectors were hanging from the ceiling with thin ropes, in order to minimize dead material and background sources close to the detector-sensitive volume. In this disposition, the MC calculated detection efficiency for $E_\gamma = 1.27$ MeV and an electronic threshold of 100 keV was $\varepsilon_\gamma = 3.3\%$ for a BICRON detector and $\varepsilon_\gamma = 4.7\%$ for a FZK detector. Fig. 2 shows a schematic drawing of the detector set-up.

Thin and thick samples of natural Fe with different diameters were used, their total number being limited by the available beam time. For normalization purposes both Au (thin and thick) and Ag samples were used, which have well-known

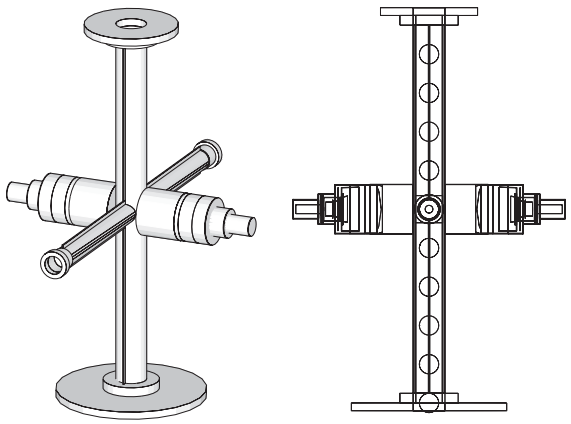

Fig. 2. Left: general view of the experimental arrangement showing the sample changer and C_6D_6 detectors. Right: details of the geometrical description as implemented in the Geant4 code.

strong resonances at $E_R = 4.9$ eV and $E_R = 5.2$ eV, respectively. The dimensions of the different samples measured for each detector set-up are given in Table 1 together with the total number of accelerator protons N_p employed in each case which is proportional to the number of neutrons incident on the sample.

The neutrons are produced through the spallation process induced by the pulses from the CERN Proton Synchrotron (PS) impinging on a Pb target with an energy of $E_p = 20$ GeV. The proton pulses having a duration of 14 ns (FWHM) and an intensity I_p in the range $3–7 \times 10^{12}$ protons per pulse, hit the target every 2.4 s (or multiples of this quantity). This very low duty cycle is one of the key features of the n_TOF installation because it not only provides the possibility to measure radioactive samples with a greatly improved signal to background ratio, but also has allowed the implementation of a zero dead time and full information preserving Data Acquisition System (DAQ) [12]. The system front end electronics is based on Flash Analog to Digital Converters (FADC) which sample and store the full analogue waveform provided by the detector (in the case of the C_6D_6 detector, the PMT anode signal) starting at the proton pulse arriving time. We have used commercial ACQIRIS 8-bit digitizers with a sampling frequency of 500 MHz and 8 MBytes of memory, allowing us to register the signals produced by neutrons arriving as late as 16 ms (equivalent to $E_n = 0.7$ eV) after the start pulse.

Table 1
Samples measured for each detector set-up

Set-up	Sample/ dimensions (mm)	Thickness (atoms/barn)	Number of protons
BICRON	Au 0.1×45	6.32×10^{-4}	1.23×10^{16}
	Fe 0.5×45	4.18×10^{-3}	2.59×10^{17}
	Ag 0.2×20	1.19×10^{-3}	8.72×10^{15}
	Au 1.0×20	5.58×10^{-3}	5.27×10^{16}
	Fe 1.5×20	1.25×10^{-2}	2.05×10^{17}
FZK	Au 0.1×45	6.32×10^{-4}	6.71×10^{15}
	Fe 0.5×45	4.18×10^{-3}	1.37×10^{17}
	Fe 2.0×45	1.71×10^{-2}	5.69×10^{17}

An on-line zero suppression system which suppresses digitized values below a given threshold and software compression allows a considerable reduction in the amount of data to be stored. The DAQ software simultaneously collects the information from all relevant detectors, monitors, etc. and sends it via a fast electronic link to the CERN Central Data Recording Facility (CDR) for permanent storage.

In order to have direct monitoring of the number of neutrons arriving at the sample a system based on the ^{6}Li(n, α)t reaction was used. Four large area Si detectors are used to detect the reaction products coming from a 200 $\mu g/cm^2$ thick and 6 cm diameter ^{6}Li deposit on a 3 μm mylar foil. The Silicon Monitor (SiMON) is installed in a vacuum chamber 2.5 m upstream from the sample changer. A preamplifier and a shaping amplifier are used to transform the detector signals before being sent to the digitizer.

The energy calibration of the C_6D_6 detector response was carried out using three reference photon sources: ^{137}Cs (0.66 MeV), ^{60}Co (1.17 and 1.33 MeV) and ^{238}Pu/^{13}C(α, n)^{16}O (6.13 MeV). The calibration in energy was obtained from a comparison of the measured energy spectra with a GEANT MC simulation of the sources. This procedure also yielded the calibration of the instrumental widening (assumed Gaussian) necessary to convolute the zero width MC responses, prior to the calculation of the WF. A linear energy calibration was found to be adequate in the case of the FZK detectors over the whole energy range, while for the BICRON detectors two different linear calibrations were used below and above 0.9 MeV. The energy dependence of the Gaussian width was found to be adequately represented by $\sigma^2_{instr} = 3E$ for the BICRON detectors and $\sigma^2_{instr} = 6E$ for the FZK detectors, when the energy is expressed in keV.

4. Results and discussion

4.1. Weighting function calculation

The WF were obtained from MC simulations of the photon response distributions for each

particular experimental set-up, with the sample itself included in the definition of the set-up. Both the GEANT3 package and the more recent Geant4 [13] package have been used to perform the simulations, in order to check for code-related systematic differences. Both codes have an adequate description of the electromagnetic processes, and the comparisons which we have made with other standard codes as MCNP and PENELOPE [14], for selected γ-ray energies and simplified geometries, show good agreement between all of them. The powerful geometry package of GEANT3 and Geant4 facilitates the implementation of the detailed geometry of the set-up, as shown in Fig. 2 for the Geant4 case. The geometrical description includes the sample changer and the detector with the PMT, although it was found that the latter has only a minor effect on the simulated response. In the case of GEANT3 the automatic tracking option (AUTO = 1) was employed since it was verified that a more detailed and time consuming tracking of the secondary electrons produces negligible differences in the response. In the case of Geant4 the Standard Electromagnetic Package was used and the tracking cut length was lowered to 0.01 mm, when a stable result was achieved.

The deposited energy distribution in the sensitive detector volume was simulated for 12 γ-ray energies E_γ in the range from 0.1 to 10.5 MeV. For each energy, 5×10^6 photons were isotropically emitted starting randomly from the sample volume with a radial probability distribution following the neutron beam profile (see Section 3). It was verified that the depth distribution had a marginal effect on the results, although in principle this distribution is very different for weak resonances (practically uniform) and strong resonances (surface peaked) in the capture measurements.

The energy spectra were histogrammed using bins of width $\Delta E = 50$ keV, convoluted with the Gaussian representing the instrumental resolution and normalized to the total efficiency to obtain R_i^j. In the upper part of Fig. 3 is shown a set of simulated responses for one of the samples. In order to obtain the weighting factors as a function of the energy W_i it was assumed that they can be adequately represented by a polynomial of

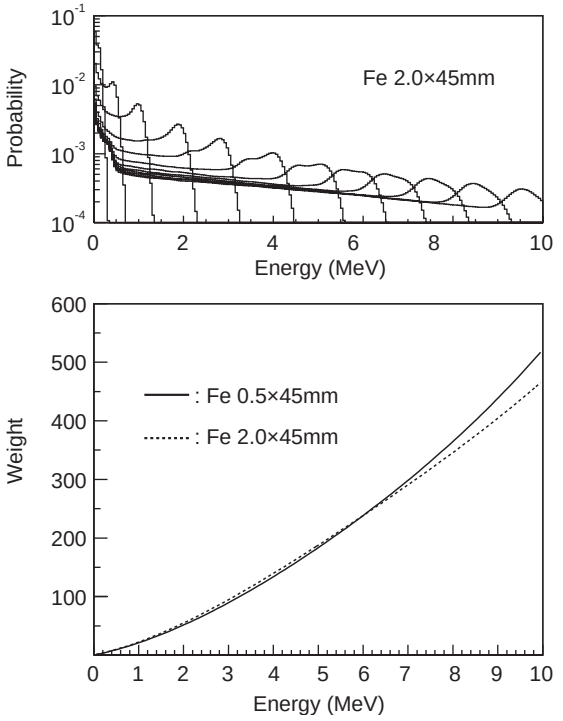

Fig. 3. Lower panel: weighting functions calculated for two different Fe samples. Upper panel: set of simulated detector response distributions for one of the samples.

degree 4, so that Eq. (3) was rewritten (taking the proportionality factor $\alpha = 1$):

$$\min \sum_{j=1}^{12} \left(\sum_{i=1}^{210} \sum_{k=0}^{4} a_k ((i-0.5)\Delta E)^k R_i^j - E_{\gamma_j} \right)^2 . \quad (4)$$

The minimization performed using the code MINUIT [15], gives the polynomial coefficients a_k. Tests were performed using a larger number of photon response distributions and/or polynomial degree, showing a negligible influence on the WF. The WF obtained for two different Fe samples are displayed in the lower part of Fig. 3, illustrating the effect of the sample size.

In order to estimate the statistical uncertainties in the WF obtained, instead of trying to introduce the covariance matrix of the simulated responses into Eq. (4), we have followed a different procedure. This consisted of simulating a large number N_c of random γ-ray cascades with a fixed cascade energy E_c using the same code employed to obtain

the mono-energetic response functions in each case, with the photons in the cascade being emitted sequentially. According to the principles of the PHWT the weighted sum of the contents N_i of the simulated energy spectra (conveniently broadened) should be equal to the product of the cascade energy and the number of cascades:

$$\sum_i W_i N_i = N_c E_c. \quad (5)$$

Therefore the deviations from this value are a measure of the uncertainty in the WF. It was verified that in all the cases the deviations were below 0.6%. The same method was used to verify the effect of the instrumental width used to convolute the MC on the WF, showing variations of a few per mil for reasonable variations of the width. A value of 0.3% will be used as the statistical uncertainty associated with the WF.

4.2. Data analysis

In order to apply the PHWT, for each registered signal the Time Of Flight (TOF) and the deposited energy have to be determined. In the case of the first set of measurements a simple analysis algorithm was used to extract this information from the data stored for each proton pulse. The digitized PMT signal is searched sequentially for values exceeding a given threshold and the time t_{start} at which the signal rises from the base line is determined. Starting from this time the signal is integrated backwards during $\Delta t = 500$ ns in order to determine the average height of the base line, and $\Delta t = 68$ ns in the forward direction to determine the total charge (after correcting for the base line). These integration time values were determined empirically to give the best energy resolution. A more time consuming analysis algorithm based on pulse shape fitting was used for the second set of measurements. It uses an experimentally determined pulse shape and a polynomial base line to obtain the integrated charge of successive pulses in an iterative fitting procedure. This algorithm was developed to handle situations of rapidly changing base line and/or high pulse pile-up rate. This is not the case for the resonances analyzed and in fact they were used to test the new algorithm, giving results consistent with the previous algorithm.

The time–charge information, together with the information from the Si monitor (see below), the pulse proton intensity and other control parameters is stored as a formatted list for further processing with the ROOT software package [16]. The time t_{start} is converted into TOF using as reference the easily identified accumulation of signals coming from photons and relativistic particles originating at the proton impact on the spallation target. The integrated charge is converted into energy using the calibration obtained from the radioactive sources. With this energy the weight is calculated from the corresponding WF and accumulated in a TOF histogram of adequate bin size. Only counts with energy larger than a given threshold are accumulated in order to eliminate the noise in the detector. The threshold used was $E_{thr} = 150$ keV for the BICRON detectors and $E_{thr} = 250$ keV for the FZK detectors. An upper energy threshold of 10 MeV was also applied as a means to reduce background counts. The histogram of weighted counts N_W is transformed into an experimental yield Y^{exp} histogram using the relation:

$$N_W = Y^{exp} N_n E_c \quad (6)$$

where N_n is the total number of neutrons arriving in the TOF bin and E_c the capture energy which represents the detection efficiency according to the PHWT. The capture energy in turn is the sum of the neutron energy E_n (obtained from the TOF) corrected for the recoil and the neutron separation energy S_n. The number of neutrons per bin was obtained from a parameterization of the neutron intensity given by $I_n = 1.522 \times 10^4 E_n^{-0.98}$ neutrons/eV per 7×10^{12} protons, with E_n expressed in eV. This parameterization fits well the preliminary data obtained from a ^{235}U fission chamber [12] in the region 1 eV–5 keV. For the samples with the small diameter (20 mm) the neutron intensity will be multiplied by a factor 0.59 obtained from the MC simulation of the neutron beam optics. As will be explained later, for the present study the precise form of this curve is not required since only relative values will be compared. The total proton pulse intensity as

registered by a beam current transformer located in front of the Pb spallation target was initially used to determine N_n from the parameterization. It was subsequently found that there were too large deviations of the beam current reading for some proton pulses and therefore the Si monitor information was used to correct the data. The digitized Si amplifier signal was analyzed to obtain the time of occurrence and amplitude (i.e. maximum value corrected for base line) of each detector pulse. The spectrum of amplitudes showed a peak corresponding to the energy deposited by tritons clearly separated from a lower broad structure produced by the alpha particles, as expected for the chosen ^{6}Li deposit thickness. The number of counts registered in the triton peak with TOF corresponding to neutron energies in the range 1 eV–10 keV was used as reference to monitor the number of incident neutrons. The alpha particle signals were not used in order to avoid the effect of the electronic threshold.

The experimental yield was analysed using the multilevel R-matrix code SAMMY [17] to fit the yield data in the relevant region around the resonance energies. The fit function used has the form

$$Y^{\exp} = A\,Y^{\text{the}} + B \tag{7}$$

where Y^{the} is the theoretical yield calculated by SAMMY, A is a normalization factor, and B a function to adjust the background shape in this region. The theoretical yield is calculated from the sample thickness and composition, and the known resonance parameters taken from data compilations [18]. It also includes several experimental effects: (i) the sample self-shielding, (ii) the broadening due to the thermal motion of atoms in the sample calculated from the temperature (which dominates the resonance width at the energies considered), (iii) the broadening due to the neutron beam resolution function, obtained from a MC simulation [12] of the spallation-moderation process induced by the proton pulses in the n_TOF target assembly, and (iv) the distortion effect of single and double neutron scattering in the sample before capture. The fit parameters are the normalization factor A and the background function B, which in fact was found to be well represented by a constant term. The resonance energy E_R was also allowed to vary in order to be independent of the accuracy of the neutron energy versus TOF calibration. We show in Fig. 4 examples of the quality of the fits achieved.

All the relevant information is contained in the yield normalization factor A given by the fitting procedure. In Table 2 we present the values of A and their uncertainty for all the samples measured using the WF calculated with GEANT3 simulated responses. In the ideal situation, this factor A should be equal to unity for a well known resonance. In practice it is affected by a number of systematic deviations including the one we are interested in: the accuracy of the WF. Therefore in order to extract information on the latter the other systematic corrections have to be accounted for.

The exact shape and absolute value of the neutron intensity versus energy distribution used to calculate the yield obviously affect the value of

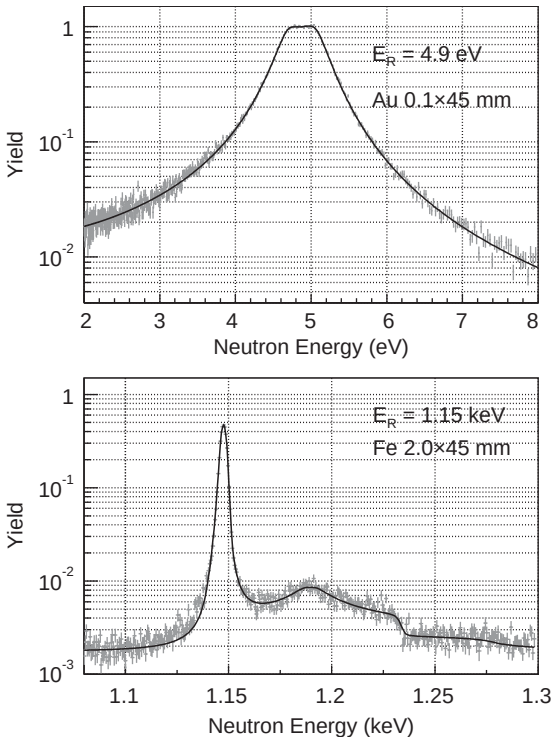

Fig. 4. Examples of the fits obtained for the saturated resonance in Au (upper panel) and the resonance in Fe (lower panel).

Table 2
SAMMY fit yield normalization factor and the correction factors for each measurement

Set-up	Sample/dimensions (mm)	E_R	A	f^{Si}	f^{thr}	A^{corr}
BICRON	Au 0.1 × 45	4.9 eV	0.811(3)	1.000(9)	1.045(4)	0.847(9)
	Fe 0.5 × 45	1.15 keV	0.780(10)	1.020(7)	1.002(4)	0.797(12)
	Ag 0.2 × 20	5.2 eV	0.812(3)	1.023(10)	1.026(4)	0.852(10)
	Au 1.0 × 20	4.9 eV	0.802(2)	0.997(7)	1.060(4)	0.847(10)
	Fe 1.5 × 20	1.15 keV	0.827(8)	1.001(7)	1.009(4)	0.835(11)
FZK	Au 0.1 × 45	4.9 eV	1.024(4)	1.000(22)	1.056(4)	1.081(25)
	Fe 0.5 × 45	1.15 keV	1.034(10)	1.011(16)	1.009(4)	1.055(20)
	Fe 2.0 × 45	1.15 keV	0.933(5)	1.084(17)	1.018(4)	1.030(18)

A. This dependence plays no role if we compare the ratios between the value for the Fe sample ($E_R = 1.15$ keV) and the value for the reference sample, since the resonance energies are very close for Au ($E_R = 4.9$ eV) and Ag ($E_R = 5.2$ eV). In this way we also eliminate other systematic effects which may affect the calculated WF but are somehow of a trivial nature, namely the exact positioning of the detector with respect to the sample or the exact volume of the liquid scintillator, which introduce only a multiplicative factor in the WF and therefore cancel out in the ratio. It should be remembered that in fact the use of a reference is the standard procedure followed to extract the cross-section in this type of experiments.

We should also consider the systematic deviation that can be introduced by a wrong C_6D_6 energy calibration. The calculated weight is quite sensitive to the energy calibration as can be deduced from Fig. 3. However, the sensitivity of the yield (accumulated weights) is reduced if values relative to a reference sample are used. The sensitivity is then related to the differences in the energy deposited spectra and WF of the measured sample with respect to the reference sample. Actually the nuclear structure and capture energy determine the spectrum of Fe ($S_n = 7.646$ MeV) to be much harder than the spectrum from Au ($S_n = 6.512$ MeV). From the fits to the energy calibration sources we can estimate the uncertainty in the slope of the calibration to be of the order of $\pm 2\%$. Changing the slope of the calibration by this amount has a negligible effect on the relative normalization factors. Even a change of 5% in the slope produces a change of only 0.3% in the relative values.

As mentioned earlier, it was found necessary to introduce a correction based on the Si monitor data to the number of neutrons arriving at each sample as calculated from the proton intensity. Since the SiMON data is not absolutely calibrated this correction is necessarily relative. Moreover since during the second set of measurements a new Li foil was employed and only two out of the four Si detectors could be used, the correction will be made relative to the thin Au sample independently for both measurements. The correction factor f^{Si} is listed in Table 2, the uncertainty being due to the statistics.

The noise rejecting threshold in the deposited energy obviously produces a loss of counts. If these counts are coming from photons for which part of the response lies above the threshold, the loss can be corrected by the WF if Eq. (4) is modified to make the summation on the energy index i starting at the threshold and not at zero energy. The loss of counts due to responses lying below the threshold can only be estimated with a model to predict such counts. It is therefore important to keep this threshold as low as possible, but it is still necessary to evaluate its effect. We have used the statistical model of the nucleus for this purpose.

An MC code was written [2] to generate γ-ray cascades from the capture resonances using levels and branching ratios obtained from the statistical model at high excitation energies and the

experimental level scheme at low excitation energies. Recommended parameters [19] were used to obtain appropriate level densities and gamma strengths for the model. The cascades are fed to the event generator of the GEANT simulation for the experimental set-up and the deposited energy spectrum is calculated. From this spectrum the weighted sum (Eq. (5)) with a given WF and threshold is calculated and normalized to the number of cascades times the cascade energy. It was mentioned earlier that this normalized sum should be equal to 1 for the correct weighting function and it was verified that indeed it agreed within 0.6% in all the cases for a threshold $E_{\mathrm{thr}} = 0$. The deviation from unity of the normalized weighted sum for a WF derived with a given threshold when the sum is performed with the same threshold measures the importance of the signals lying below that threshold. From the simulations it was found that this effect amounts to about 0.5% for the Fe samples and about 3% for the reference samples (Au, Ag) when the threshold was 150 keV and 1.5% and 5%, respectively when the threshold was 250 keV.

These simulations were made sending the γ-rays in the cascade sequentially in order to avoid that more than one of them hit a detector. Due to the non-negligible value of the detector efficiency there is always a certain possibility that two (or more) γ-rays from the cascade leave part of their energy simultaneously. If the WF was strictly proportional to the energy this summing effect would not produce any distortion. As can be appreciated in Fig. 3, in general the weighting function is a convex function, so that the weight of the summed signal is larger than the sum of the weights of the individual signals. The final effect depends on the γ-ray cascade energy and multiplicity distribution. Again the statistical model of the nucleus provides a realistic description of these quantities. The effect can be quantified comparing a simulation in which the photons in the cascade are emitted simultaneously to a simulation where these are emitted sequentially. It was found that the effect lies between 1% and 2% in all cases.

The Conversion Electron (CE) process substitutes γ-rays in the cascade with less-penetrating electrons and X-rays leading to a loss of registered counts. In particular it is known [20] that the level scheme of ^{198}Au at low excitation energy includes several strongly converted transitions, and since gold is frequently used as a reference sample, the study of this effect was relevant. The CE process is more important for very low-energy transitions, and some of them would have been lost anyhow because of the existence of the electronic threshold, except that there is some possibility for the γ-ray signals below the threshold to be summed and contribute to the weight. The importance of the effect also depends on the probability that strongly converted transitions form part of the cascade. Therefore it was decided to include a model [2] of the CE process for selected transitions in the capture cascade generator code. The process could be activated for known converted transitions in the experimental level scheme used at low excitation energies. In this way a comparison of simulations with and without the CE process gives us an estimate of the effect. It was found that for the thresholds used the differences were negligible even for Au.

We include in Table 2 the correction factor f^{thr} due to the combined effect of summing, CE processes and low-energy transitions for the given energy threshold as estimated from the MC simulations of the measurement. The uncertainty given is just the statistical uncertainty of the normalized weighted sum. It is not easy to assign a value for the systematic (model dependent) uncertainty associated with this correction, but in view of the magnitude of the corrections a value of 1% was assumed.

The corrected yield normalization factor, taking into account the SiMON correction on the neutron intensity and the correction due to the electronic threshold: $A^{\mathrm{corr}} = f^{\mathrm{Si}} f^{\mathrm{thr}} A$, is given in the last column of Table 2. The uncertainty quoted also includes the 0.3% statistical uncertainty from the weighting function plus the assumed 1% uncertainty from the threshold correction method. In Table 3 the values of the corrected normalization factor for the 1.15 keV resonance in ^{56}Fe relative to the respective reference sample values A^{rel} are given for the different sample/reference sample combinations. The fact that these values are consistently lower than unity, with an average

value of 0.967, can be viewed as an indication that the relative neutron flux at 1.15 keV with respect to the flux at 5 eV is 3.3% lower than we have obtained from the preliminary flux data. Consistent with this interpretation the results presented in Fig. 5 have been normalized to the average value of 0.967, although it has to be stressed that this will not affect our conclusions. This figure shows the uncertainty with which the integrated yield of the 1.15 keV resonance could be determined. All the values including those corresponding to thick samples agree within the error bars (2–3%), and their RMS deviation is 1.7%. In a similar analysis performed using the WF calculated from the Geant4 simulations, it was found that the results agree with those in the figure within 1%. It can be concluded that the PHWT with WF obtained from detailed MC simulations of the sample-detector set-up can determine the reaction yield with an accuracy of 2% or better. The results in Fig. 5 can be compared to the experimental results obtained by Fioni et al. [9] shown in Fig. 1, evidencing that the GEANT MC simulation is able to take into account properly the influence of the sample dimensions on the detector response.

Table 3
Corrected yield normalization factors for the 1.15 keV resonance in ^{56}Fe relative to the reference sample

Set-up	Sample/reference sample	A^{rel}
BICRON	Fe 0.5 mm/Au 0.1 mm	0.941(22)
	Fe 1.5 mm/Au 0.1 mm	0.980(22)
	Fe 1.5 mm/Au 1.0 mm	0.985(21)
FZK	Fe 0.5 mm/Au 0.1 mm	0.975(32)
	Fe 2.0 mm/Au 0.1 mm	0.952(30)

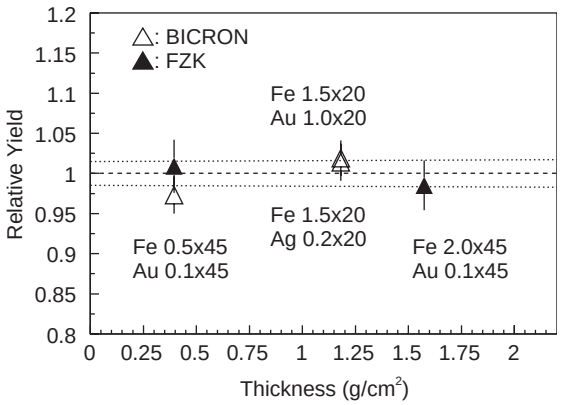

Fig. 5. Relative reaction yields obtained in this work for the 1.15 keV resonance in ^{56}Fe using different experimental set-ups. The RMS deviation of the points is indicated (dotted line).

5. Summary and conclusions

We have investigated the reliability of the pulse height weighting technique (PHWT) for the determination of neutron capture cross-sections, in particular the ability to produce consistent results using different sample sizes and detector set-ups. The only practical way to take into account these differences in the detector response is to use Monte Carlo (MC) simulations to obtain the energy-dependent weighting factors. The GEANT3 and Geant4 simulation codes were tested against selected measurements. The 1.15 keV resonance in ^{56}Fe which was found particularly sensitive in the past, was chosen for this purpose. The measurements were performed with two different types of C_6D_6 liquid scintillation detectors using different sample thicknesses and diameters. Sources of systematic deviation were carefully investigated and accounted for. As a result it was determined that the resonance-integrated yield in all cases agreed within the error bars with an RMS deviation of 1.7%, and no sample size dependence was observed. It is concluded therefore that the PHWT applied to C_6D_6 data with MC calculated weighting factors is able to achieve an accuracy of 2% or better.

Acknowledgements

Research supported by the European Commission (FIKW-CT-2000-00107), by the Spanish Ministry of Science and Technology (FPA2001-0144-C05) and by the Austrian Ministry of Education, Science and Culture (GZ650.645/1-VI/1a/2002). This work is part of the Ph.D. thesis of C. Domingo-Pardo who acknowledges a I3P-

FSE fellowship from Consejo Superior de Investigaciones Científicas.

References

[1] The n_TOF Collaboration, European collaboration for high-resolution measurements of neutron cross sections between 1 eV and 250 MeV, CERN-SPSC-99-8/SPSC-P-310, CERN, 1999.
[2] J.L. Tain, et al., J. Nucl. Sci. Tech., Suppl. 2 (2002) 689.
[3] R.L. Macklin, J.H. Gibbons, Phys. Rev. 159 (1967) 1007.
[4] F. Corvi, et al., Nucl. Sci. Eng. 107 (1991) 272.
[5] F.G. Perey, et al., Proceedings of the International Conference on Nuclear Data for Science and Technology, Mito, Japan, 30 May–3 June 1988, p. 379.
[6] W.R. Nelson, H. Hirayama, D.W.O. Rogers, The EGS4 code system, SLAC-265, Stanford Linear Accelerator Center, 1985.
[7] GEANT: Detector description and simulation tool, CERN Program Library W5013, 1994.
[8] J.F. Briesmeister (Ed.), MCNP—a general Monte Carlo N-particle transport code, Version 4B, LA-12625-M, 1997.
[9] G. Fioni, Ph.D. Thesis, Gent University, Belgium, 1991; F. Corvi, et al., in: S.M. Qaim (Ed.), Nuclear Data for Science and Technology, Springer, Berlin, 1992, p. 44.
[10] R. Plag, et al., Nucl. Instr. and Meth. A 496 (2003) 425.
[11] The n_TOF Collaboration, Technical Report, CERN/INTC-2000-018, CERN, 2000.
[12] The n_TOF Collaboration, Performance Report, CERN/INTC-2002-037, CERN, 2002.
[13] Agostinelli, et al., Nucl. Instr. and Meth. A 506 (2003) 250.
[14] F. Salvat, et al., PENELOPE—a code system for Monte Carlo simulation of electron and photon transport, NEA/NSC/DOC-2001-19, 2001.
[15] F. James, MINUIT—function minimization and error analysis, CERN Program Library, CERN, 1994.
[16] R. Brun, F. Rademakers, ROOT—an object oriented data analysis framework, Proceedings AIHENP'96 Workshop, Lausanne, September 1996, Nucl. Instr. and Meth. A 389 (1997) 81.
[17] N. Larson, A code system for multilevel R-matrix fits to neutron data using bayes equations, ORNL/TM-9179/R5, 2000.
[18] Cross Section Evaluation Working Group, ENDF/B-VI Summary Documentation, BNL-NCS-17541 (ENDF-201), 1991.
[19] Reference Input Parameter Library—Handbook for Calculations of Nuclear Reaction Data, IAEA-TECDOC-1034, 1998.
[20] M.R. Bhat, Evaluated nuclear structure data file (ENSDF), in: S.M. Qaim (Ed.), Nuclear Data For Science and Technology, Springer, Berlin, 1992, p. 817.